

UDC 552.26+551.25

**M. A. HASSAN**, Lecturer in the Department of Geology<sup>1</sup>, Post-Graduate Student<sup>2</sup>, musabeljah78@gmail.com  
**A. E. KOTELNIKOV**<sup>2</sup>, Head of the Department of mineral developing and oil & gas engineering, Associate Professor, Candidate of Geologo-Mineralogical Sciences  
**E. A. ABDULLAH**<sup>2</sup>, Assistant of the Department of mineral developing and oil&gas engineering  
**E. M. KOTELNIKOVA**<sup>2</sup>, Senior Lecturer, Candidate of Geologo-Mineralogical Sciences

<sup>1</sup> Faculty of Petroleum and Minerals – Al Neelain University, Khartoum, Sudan

<sup>2</sup> Academy of Engineering, Peoples' Friendship University of Russia – RUDN University, Moscow, Russia

## MINERAL CHEMISTRY AND PETROLOGY OF MANTLE PERIDOTITES FROM THE QALA EN NAHAL-UMM SAQATA OPHIOLITE, GEDARIF STATE, SUDAN

### Introduction

Recently, a number of ophiolite complexes have been recognized in the Proterozoic terranes. The Late Proterozoic Nubian- Arabian Shield (NAS), which is part of the NE African Orogen, formed between 900 – 550Ma [1–4], hosts a number of ophiolite complexes, which furnish one of the highest ophiolite densities known for a Proterozoic terrain on the planet [5]. Other studies of this territory that we carried out in the article [6]. The predecessors studied the ophiolite complexes of Saudi Arabia, the Eastern Desert of Egypt, Kenya, and eastern Sudan.

### Geologic setting and field observations

The study area is located some 70 km to the southwest of the Gedarif city, Gedarif State, in eastern Sudan. Mostly the area is composed of exposed crystalline metamorphic rocks of the Precambrian Basement Complex, and there are separate outcrops of Tertiary volcanic and Mesozoic sedimentary rocks (Nubian Sandstone Formation). The area can be classified in to two tectono-stratigraphic terranes based on the differences in metamorphic grades and on the structural style: (1) high-grade schists and gneiss terrane and (2) ophiolitic fold and thrust belt, known as Qala-En Nahal-Umm Saqata ophiolitic complex, which is structurally overlying a layered sequence of low-grade metavolcano-sedimentary units. The granites (syn-, late- and post-orogenic) intrude the above-mentioned sequences and usually form a conspicuous, hilly dissected massifs (**fig. 1**).

The mafic-ultramafic ophiolite complex has been thrust over the low-grade metavolcano-sedimentary rocks. The assemblages are consisting of serpentinitized ultramafic rocks (mainly harzburgite with subordinate minor dunite), mafic-ultramafic cumulate rocks (composed of layered gabbros and pyroxenites), massive gabbro and associated plagiogranites and a volcanic complex composed of massive to pillow-basalts and sheeted dolerite dykes.

The relatively large-scale exposed masses of mantle peridotites include mainly the Utash mass and the Umm Saqata mass in the south and the Qala en Nahal mass and the Fau mass in the north of the study area.

The mantle peridotites are mainly serpentinites, with talc-carbonates and chlorite schists restricted to the fault zones, either within or marginal to the ultramafic bodies. These

*The study area of this research some 70 km southwest of Gedarif city, Gedarif State, in eastern Sudan. With a geological position, it is located within two major lithological associations, representing two different crustal entities: Saharan Metacraton (SMC) in the west and the Arabian Nubian Shield (ANS) to the east. The main objective of the study is a petrological investigation of the mantle peridotites within Qala En Nahal-Umm Saqata area. The relatively large-scale exposed masses of mantle's peridotite, include mainly the Utash mass and the Umm Saqata mass in the south and the Qala en Nahal mass and the Fau mass in the north of the area. Petrographically, they are mostly serpentinite. They have low-contents of  $Al_2O_3$ ,  $CaO$ ,  $TiO_2$ ,  $MgO$ ,  $Na_2O$  and  $K_2O$ , all consistent with depleted mantle materials, and similar to the metamorphic peridotites. The analyzed serpentine minerals are mainly pseudomorphic serpentines with subordinate antigorite, which may suggest that the parent minerals were first retrogressed to form lizardite and chrysotile. Subsequently, progressive metamorphism has recrystallized these minerals into antigorite. The chromites from the study area have high Cr# (Cr# varies from 0.51 to 0.87), most probably representing the primary phase which is similar to chromian spinels in mantle-derived peridotites. The presence of podiform chromites in the studied serpentinites is a typical of supra-subduction ophiolites, with Cr# similar to those of forearc ophiolites and boninite-derived chromites. Qala En Nahal-Umm Saqata mantle peridotites were formed in a forearc setting, during the subduction initiation that developed as a result of southeastward-dipping subduction zone. They possibly represent ensimatic, thrust material, after the collision of the Nubian-Arabian Shield with the older sialic continental Saharan Metacraton during the late Proterozoic, Pan-African tectono-thermal event.*

**Keywords:** Qala En Nahal-Umm Saqata, Sudan, mineral chemistry, petrology, peridotite, ophiolite, serpentinite, chromite, supra subduction zone, forearc.

**DOI:** 10.17580/em.2021.01.03

mantle peridotites are in structural contact with the adjacent country rocks. There is no evidence of magmatic emplacement, since there are no dykes from the bodies into the country rocks, no chilled margins or contact metamorphic aureoles around these bodies. The serpentinites of the mantle peridotites (basal ultramafic teconites) were later subjected to hydrothermal alteration, resulting in the formation of talc carbonate and listvenite (quartz carbonate). Secondary silicification of these serpentinites (birbirites) is common, especially at the crest of the hills where it is produced by differential weathering. These serpentinite rocks are converted into talc schists along shear zones. The presence of low-angle zones of chlorite schist with well-developed crystals of magnetite and talc carbonate schist are indicative of thrusting environment [7]. The serpentinite rocks are also cut by stock works and/or veins of magnesite occurring.



Fig. 1. Geological map of the study area

### Petrography

The mantle peridotites are mostly serpentized [8]. In the study area the serpentinites are shown as smooth feel, various shades of green, ranging from dull-grayish-to dark green, with weather reddish brown colour. It is generally massive, but become sheared and foliated at the base near the thrust planes or shear zones where they are replaced by chlorite schists and talc-carbonate rocks. Due to the almost complete serpentization of many samples it is more correct to apply the term serpentinites for most of these rocks. Classification of these serpentinites by using the relics of primary magmatic minerals (based on modal composition) is not achievable in such cases. Therefore, geochemical data must be used to characterize the protolith of these rocks.

Pseudomorph and nonpseudomorph types [9, 10] of the serpentinites are exist in the examined sections. In the former, the serpentine occurs as a direct pseudomorph of the primary silicates. While in the latter, the serpentinite fabrics are unrelated to the primary textures in the ultramafic precursor. Pseudomorph replacement do not only preserves the outlines of the original grains and their primary textures, but may also preserve the fracture patterns and cleavages of replaced minerals.

Generally, the great majorities of pseudomorph textures, such as mesh texture are produced after olivine; while bastites are formed after pyroxene, amphibole and various layered-silicates [9]. The studied serpentinites rarely exhibit pseudomorph texture such as mesh texture and to a lesser degree few bastite texture which indicates dunite and harzburgite parental rock.

Microscopically, it shows a mesh texture, the mesh rims being chrysotile or lizardite and the mesh centers being serpophite. It has a foliatoblastic texture, formed mainly of antigorite (fig. 2a). The bastite serpentine retained the shape and the cleavage of the pyroxene. The middle of crystals are occupied by gray or brownish isotropic materials (serpophite) in contrast to the elongate blades of serpentine (fig. 2b). Beside the pseudomorph textures, many of the serpentinites exhibit non-pseudomorph textures (fig. 2c). It's illustrated by the presence of antigorite serpentine, which is formed by the recrystallization of pseudomorph serpentine (lizardite with minor concentration of chrysotile). Such phenomena was reported elsewhere

during progressive metamorphism [11]. Chrysotile is less abundant and occurs as cross-fiber veinlets traversing the antigorite matrix (fig. 2d), which indicates its late crystallization under static conditions. Opaque minerals include magnetite and chromite which occur as disseminated sub-hedral grains sometimes altered along the borders and cracks. Magnetite occurs as minute crystals or in the form of elongate crystals within the serpentinite. It is commonly associated with the mesh serpentine and concentrated along the mesh rims. Magnesite occurs as granular aggregates and discrete rhombs, or as veins or veinlets cutting the serpentine groundmass. Talc occurs as fine flakes of high interference color.

### Analytical method

After the examination of 40 thin sections prepared from the mantle peridotites, ten fairly fresh or somewhat less altered samples were selected for geochemical analysis in order to decipher their geochemical affinity and their geotectonic setting. The major and a range of trace elements were analyzed, at ALS laboratories, Saudi Arabia.

Major and minor elements (Si, Ti, Al, Cr, Fe, Mn, Mg, Ca, Na, K, P) were analyzed by mixing a 0.66 g aliquot of sample with lithium borate flux ( $\text{LiBO}_2$ ,  $\text{LiB}_4\text{O}_7$  and  $\text{LiNO}_3$ ) in 1:10 ratio, and then fusing the mixture at 1025C and pouring it into a platinum mould. The resulting disc was analyzed by X-ray fluorescence spectrometry (XRF, their method ME-XRF26). LOI was determined by thermogravimetric analysis (their ME-GRA05). For resistive trace elements (Cr, V, Cs, Rb, Ba, Sr, Th, U, Nb, Zr, Hf, Y, La, Ce, Pr, Nd, Sm, Eu, Gd, Tb, Dy, Ho, Er, Tm, Yb and Lu), an aliquot of the sample was mixed with lithium borate and fused, then digested in acid and analyzed by inductively coupled plasma mass spectrometry (ICP-MS; method ME-MS81). For base metals (Co, Cu, Ni, Sc and Zn) an aliquot of the sample was digested in a mixture of four acids ( $\text{HClO}_4$ ,  $\text{HNO}_3$ , HF and HCl) and then analyzed by inductively coupled plasma atomic emission spectrometry (ICP-AES; ME-4ACD81).

Chemical compositions of the essential rock-forming minerals in the studied mantle peridotite samples were determined by electron microprobe analysis, using a JEOL JXA-8200 equipped with five wavelength spectrometers and an energy dispersive spectrometer at the IGEM RAS, Moscow, Russia.

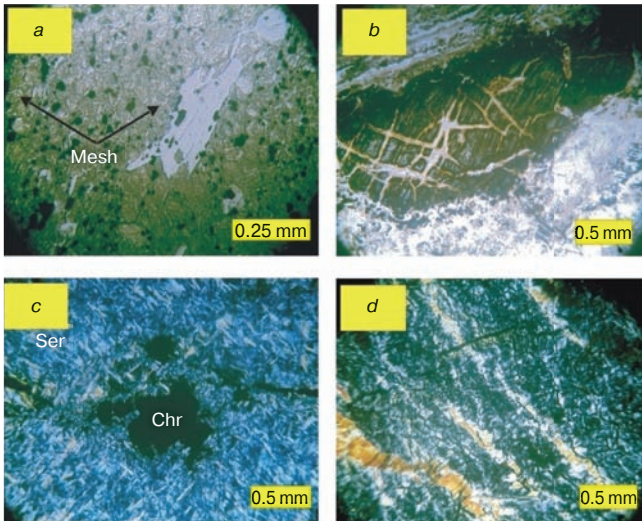


**Fig. 2. Photomicrographs showing:** (a) mesh texture produced after olivine; while (b) bastites are formed after pyroxene; (c) non-pseudomorphic textures represented by antigorite serpentinite; (d) cross-fiber veinlets of chrysotile traversing the antigorite matrix

**Results**

**Major oxides.** The chemical analyses of the mantle peridotites show a wide variation in SiO<sub>2</sub> (31.86–42.04 wt. %), MgO (33.9–39.3 wt %), Fe<sub>2</sub>O<sub>3</sub> (6.04–10.5 wt %). Mg number ranges from 0.78 to 0.88 with an average of 0.83. This average is generally close to the average ratio for the metamorphic lherzolites (0.84) and metamorphic harzburgites (0.85) given by Coleman (1977) [11]. They are depleted in Al<sub>2</sub>O<sub>3</sub>, CaO, TiO<sub>2</sub>, MnO, P<sub>2</sub>O<sub>5</sub> and alkalis. The low contents of Al<sub>2</sub>O<sub>3</sub>, CaO, TiO<sub>2</sub>, MgO, Na<sub>2</sub>O and K<sub>2</sub>O represent depleted mantle materials, and similar to the metamorphic peridotites which are considerably depleted in these elements [11].

On the Opx-Ol-Cpx triangular diagram devised by Coleman (1977) [11] in order to classify the ultrabasic rocks. The majority of the mantle peridotites plot in the harzburgite field (fig. 3a). The analyzed mantle peridotites plot within the field of metamorphic peridotites associated with ophiolites (fig. 3b). Li et al. (2004) [12] used the CaO-Al<sub>2</sub>O<sub>3</sub>-MgO diagram in order to classify the ultramafic rocks (serpentinites) into three groups of mantle protoliths. These groups are (a)

harzburgite-dunite protoliths (b) spinel-harzburgite protoliths and (c) lherzolite and spinel lherzolite protoliths. Using the same plot, the studied rocks plot in the harzburgite-dunite protolith field (fig. 3c).

**Trace and REE composition.** Trace elements distribution analysis of studied mantle peridotites, normalized to primitive upper mantle [13], shows that they are a depleted in lithophile trace elements especially HFSE. Nevertheless, they show variable relative enrichment in the most of incompatible trace elements (Rb, Ba, U and La). The REE patterns of the studied peridotites has an overall lower-HREE abundances and display relatively flat REE to concave-up normalized chondrite-normalized REE pattern [14].

**Mineral chemistry**

**Serpentine minerals.** The serpentine minerals contain 43.52–48.28 wt% SiO<sub>2</sub>, 0–2.16 wt% Al<sub>2</sub>O<sub>3</sub> and 1–3.47 wt% FeO. Due to different generations of serpentinization, the serpentinite minerals are highly variable in their compositions [15]. There are two major petrological types of serpentinite, each is distinct in its mineralogy, texture and petrogenesis [16]. The most abundant type consists of serpentinites formed by the hydration of peridotites, which is referred to here as pseudomorphic serpentinites. Their serpentine mineralogy is lizardite plus minor chrysotile, and they are characterized by textures that are strictly indicative of retrograde replacement of olivine, orthopyroxene, clino-pyroxene and, more rarely, tremolite, talc and anthophyllite. Antigorite serpentinites formed largely by recrystallization of pseudomorphic serpentinites during progressive metamorphism [9, 16]. On the MgO versus SiO<sub>2</sub> diagram (fig. 4a), the analyzed serpentine minerals are mainly pseudomorphic serpentines with subordinate antigorite serpentines, which indicates that the parent minerals were first retrogressed to form lizardite and chrysotile. Progressive metamorphism has recrystallized these minerals into antigorite. On the Cr<sub>2</sub>O<sub>3</sub> versus Al<sub>2</sub>O<sub>3</sub> diagram (fig. 4b) the analyzed serpentine minerals show variable contents of Al<sub>2</sub>O<sub>3</sub> and Cr<sub>2</sub>O<sub>3</sub> comparing to the composition of Ol-mesh, Opx-bastite and Cpx-bastite serpentines. This is interpreted to suggest their derivation from dunite and harzburgite. On the MgO versus SiO<sub>2</sub> diagram after Wicks and Plant (1979), the analyzed serpentine minerals are plotted in the field characteristic for prograde-metamorphism (fig. 4c), in which antigorite with interpenetrating texture is formed at low temperature.

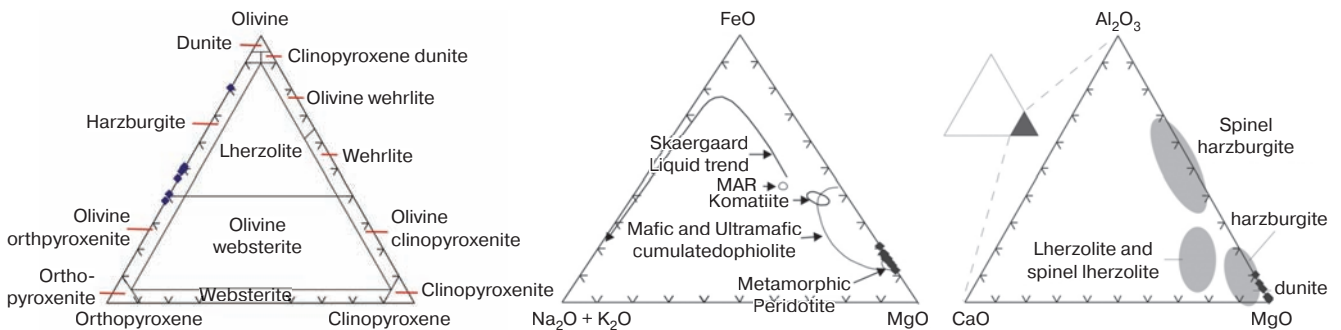


**Fig. 3. Triangular diagrams:** (a) Ol-Cpx-Opx [11] normative composition of the studied mantle peridotites; (b) FeO-MgO-(Na<sub>2</sub>O+K<sub>2</sub>O) diagram [11] for the studied mantle peridotites; (c) relationship between mantle peridotites and their protoliths [12]



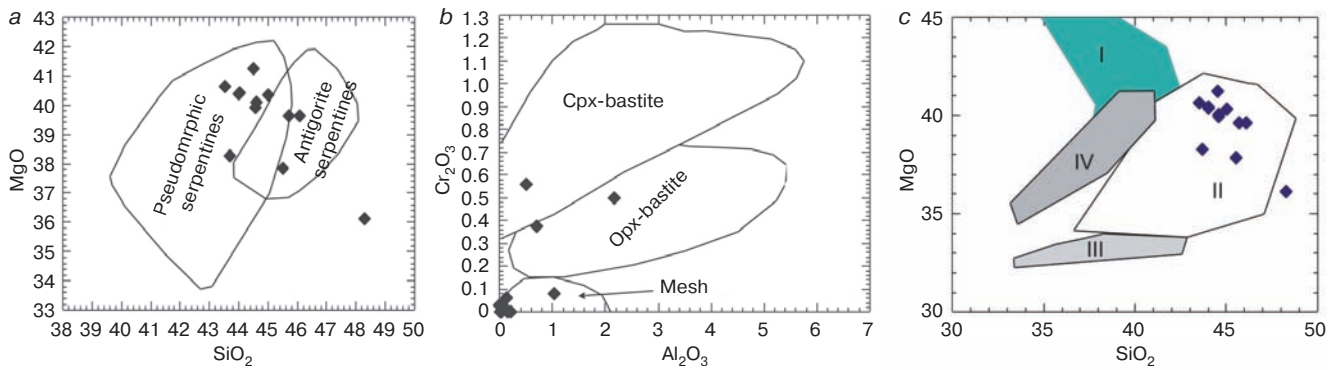


**Fig. 4. Diagrams of the analyzed serpentine minerals:**

(a) MgO versus SiO<sub>2</sub> (adapted from Dungan, 1979 [17]); (b) Cr<sub>2</sub>O<sub>3</sub> versus Al<sub>2</sub>O<sub>3</sub> (adapted from Dungan, 1979 [17]); (c) MgO versus SiO<sub>2</sub> [18]. I – Lizardite after magmatic olivine; II – Antigorite with interpearatrig texture; III – Antigorite with hourglass texture, IV – Lizardite after metamorphic olivine

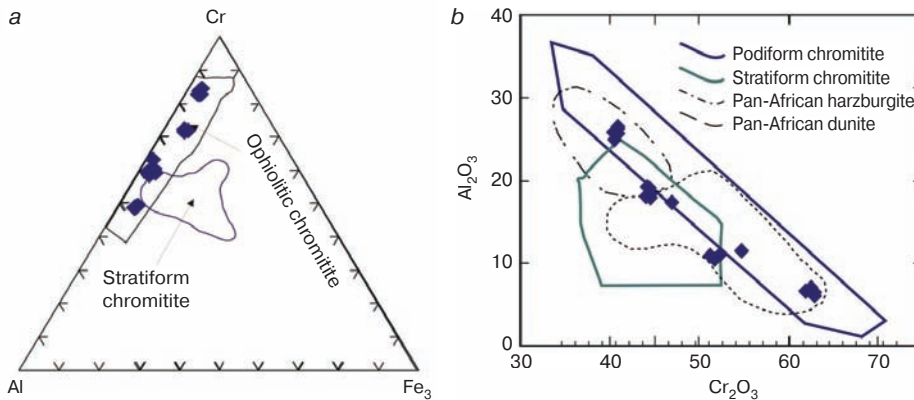


**Fig. 5. Diagrams of the analyzed chromite:**

(a) Cr-Al-Fe+3 atomic ratios diagram. The boundaries between stratiform and podiform chromitites are from Aria et al. [24] and Ferrario & Garuti [25]; (b) Al<sub>2</sub>O<sub>3</sub> vs Cr<sub>2</sub>O<sub>3</sub>. Fields are after Bonavia et al. [23]

**Chromite.** Because many of the chromite crystals are metamorphosed and altered to magnetite, only the primary chromite crystals were selected. Representative analyses for the primary chromite crystals are given in Table 3. In the completely serpentinized ultramafic rocks, which contains no relicts of primary silicate minerals, the composition of the unaltered accessory chromite is extensively used as a petrogenetic and geotectonic indicator [19]. Chromite is the only igneous mineral that retains most of its original igneous chemistry in metamorphosed serpentinites [15].

The analyzed mineral has high-Cr# [Cr/ (Cr+Al)] varying from 0.51 to 0.87 (average 0.67). Mg# [Mg/ (Mg+Fe+2)] varying from 0.13 to 0.57. This large variation is probably due to the widespread talc carbonate alteration and the fact that chromite equilibrates with abundant metamorphic carbonate minerals. This also reported elsewhere by Barnes (2000) [20]. Also, the analyzed chromites have Fe<sup>+3</sup># [Fe<sup>+3</sup>/ (Fe<sup>+3</sup>+Cr+Al)] ranges between 0.05–0.19 which are similar to podiform chromite [21], and therefore plot in the ophiolitic chromitite field in the Al-Cr-Fe<sup>+3</sup> diagram (fig. 5a). As previously indicated, the chromites have high Cr#, representing most probably the primary phase which is similar to chromian spinels in mantle-derived peridotites [22]. The majority of the analyzed chromite are low in Al relative to Cr and are similar to ophiolitic podiform chromites, particularly those associated with the harzburgite and dunite [23–25] (fig. 5b).

**Tectonic setting**

Floyd [26] has distinguished the tectonic setting of the peridotite based on petrological and geochemical grounds as (1) rift to passive margin peridotites, (2) mid – ocean ridge peridotites, (3) intra – plate peridotites, and (4) active margin peridotites. Also, Bonatti and Michael [27] have distinguished between peridotites of different tectonic settings based on Al<sub>2</sub>O<sub>3</sub> content in the whole-rock and mineral chemistry, because Al appears to be relatively unaffected by serpentinization and metamorphism. Al<sub>2</sub>O<sub>3</sub> content in the peridotites decreases from intracontinental (pre-oceanic) rifts to passive margins to mature ocean to subduction zones. The studied serpentinites have Al<sub>2</sub>O<sub>3</sub> concentrations (0.25–3.73 wt. %) that are akin to oceanic and active margin peridotites and Pan-African serpentinites (fig. 6a).

The Al<sub>2</sub>O<sub>3</sub> and CaO depletion characterize fore-arc peridotites. On the Al<sub>2</sub>O<sub>3</sub> versus CaO diagram [29], the majority of the analyzed mantle peridotites plot in the fore-arc peridotites field (fig. 6b). The Cr vs. TiO<sub>2</sub> diagram [30] also supports the SSZ setting for the studied mantle peridotite (fig. 6c).

On the TiO<sub>2</sub> versus Cr# diagram [19, 24, 32], most of the analyzed accessory chromite minerals plot in the depleted mantle peridotite and the boninite fields (fig. 6d), indicating a supra-subduction setting specially for those associated with fore arc basin.

As pointed earlier, the chromites from the study area have high Cr# values representing most probably the primary

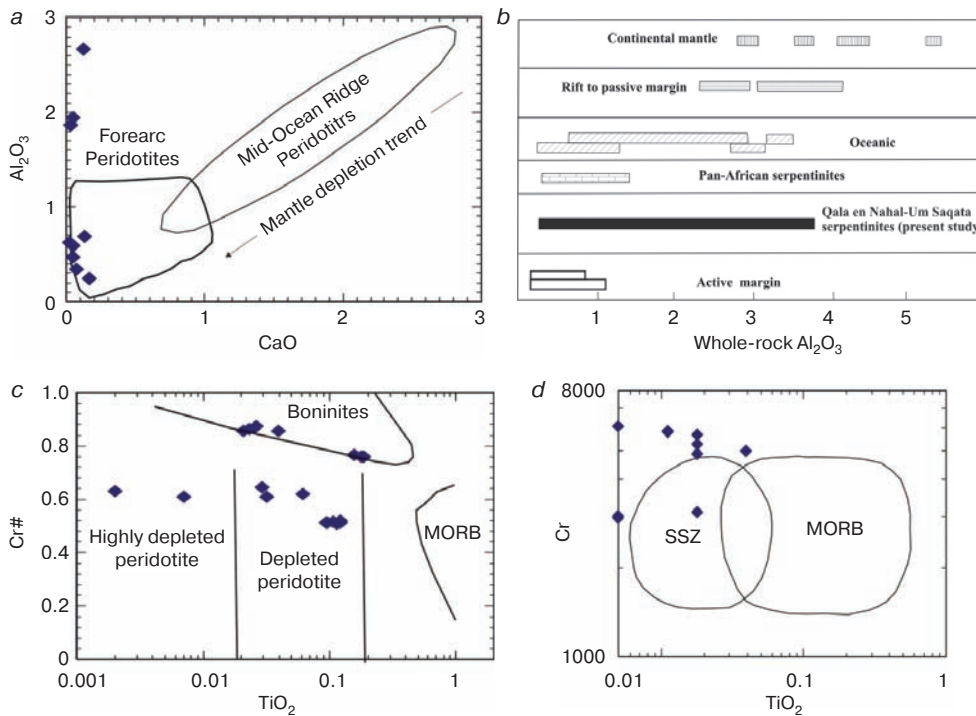


**Fig. 6. (a)**  $\text{Al}_2\text{O}_3$  contents of the whole-rock of the studied serpentinites (from Floyd [26]), the  $\text{Al}_2\text{O}_3$  of the Pan-African serpentinites adopted from El Bahariya and Arai [28]; **(b)**  $\text{Al}_2\text{O}_3$  versus CaO diagram, peridotites of the study area fall in the forearc peridotites (after Ishii et al. [29]); **(c)** Cr versus  $\text{TiO}_2$  diagram for the studied serpentinites (Pearce et al. [30]); **(d)** Cr# versus  $\text{TiO}_2$  diagram for the analyzed accessory chromite (fields after Dick and Bullen [19]; Arai [24])

phase, which is similar to chromian spinels in mantle-derived peridotites [22]. They are low in Al relative to Cr and are similar to ophiolitic podiform chromites.

Because the composition of chromian spinels is related to the degree of partial melting of their mantle source rocks, chromite is suitable for tectonic classification of peridotites and ophiolitic complexes [19, 33]. According to Dick and Bullen (1984) [19] if Cr# is less than 0.6, an abyssal peridotitic composition (Type I) and MOR-type genesis is indicated; if  $\text{Cr}\# > 0.6$  (i.e. Type I) a sub-volcanic arc (supra-subduction zone) setting is considered, and if Cr# span the full range of the two settings above then a composite origin of such ophiolite is inferred.

In the Cr# Vs Mg# (fig. 7a) the majority of studied chromites (Cr# varies from 0.51 to 0.87) plotted in forearc and boninite fields. This boninitic affinity indicates a suprasubduction setting [19, 27]. Most boninites were found in the fore-arcs of the interoceanic arcs [34–36]. The analyzed primary chromites of the study area lie in the supra-subduction zone field (fig 7b). Suprasubduction ophiolites could form either in forearcs during an incipient stage of subduction initiation or in back-arc basins [37]. Al-rich chromites are considered to form from tholeiitic melts [38] close to the composition of the back-arc basin basalts BABB [22, 39], whereas Cr-rich chromites are considered to form from boninitic melts [38]. Moreover, most of chromites have  $\text{Cr}\# > 0.6$  comparable to chromites from modern forearcs and distinctly higher than those from mid-ocean ridge (MOR) and back-arc basin peridotites.

From the geological, geochemical and mineralogical results and the geographic distribution of the metavolcanic rocks and the existence of ophiolitic rocks, we propose that the Qala en Nahal-Umm Saqata mantle peridotites were formed in a fore arc setting. This has happened during the subduction initiation which was developed as a result of southeastward-dipping subduction zone and possibly represent ensimatic, thrust material after the collision of the Nubian-Arabian Shield with

the older sialic continental Saharan Metacraton during the late Proterozoic, Pan-African tectono-thermal event.

### Conclusions

The mantle peridotite are mainly serpentinites, with talc-carbonates and chlorite schists restricted to the fault zones, either within or marginal to the ultramafic bodies. There is no evidence of magmatic emplacement, since there are no dykes from the bodies into the country rocks, no chilled margins or contact metamorphic aureoles around these bodies. The serpentinites are composed almost exclusively of minerals of the serpentine group formed by the hydrothermal alteration of the previously existing olivines and pyroxenes of the ultramafic rocks. The serpentinites rarely exhibit pseudomorphic texture such as mesh texture and to a lesser degree few bastite texture which indicates dunite and harzburgite parental rock. Beside the pseudomorphic textures many of the serpentinites exhibit non-pseudomorphic textures. This is represented by antigorite serpentine, which is formed by the recrystallization of pseudomorphic serpentine (composed of lizardite with minor concentration of chrysotile), as reported elsewhere during progressive metamorphism. Chrysotile is less abundant and occurs as cross-fiber veinlets traversing the antigorite matrix, which indicates its late crystallization under static conditions.

They are depleted in  $\text{Al}_2\text{O}_3$ , CaO,  $\text{TiO}_2$ , MnO,  $\text{P}_2\text{O}_5$  and alkalis. The low contents of  $\text{Al}_2\text{O}_3$ , CaO,  $\text{TiO}_2$ , MgO,  $\text{Na}_2\text{O}$  and  $\text{K}_2\text{O}$  represent depleted mantle materials, and similar to the metamorphic peridotites which are considerably depleted in these elements [16]. They are a depleted in terms of lithophile trace elements especially HFSE. Nevertheless, they show variable relative enrichment in the most of incompatible trace elements (Rb, Ba, U and La). LILE enrichment, which is probably associated with seawater alteration or fluids produced by dehydration of subducted slab [43, 44]. The strong relative enrichments in large ion lithophile elements (LILE),

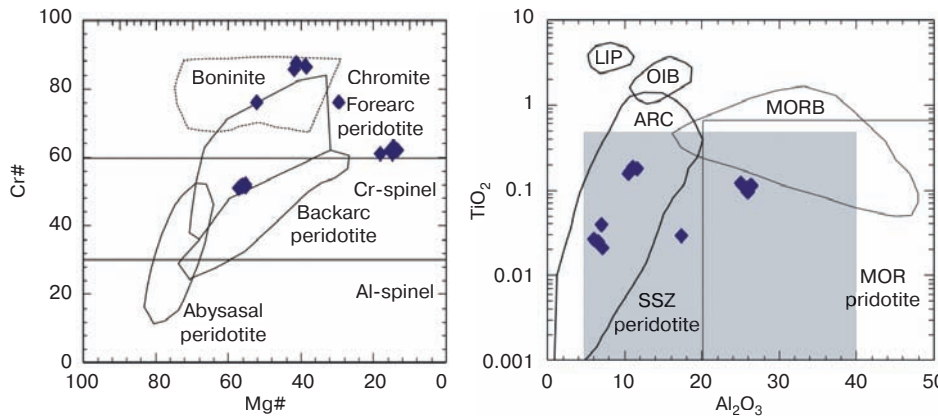


**Fig 7. (a) Cr# vs. Mg# diagram. Compositional fields for spinel-group minerals in boninite after Barnes and Roeder [40] and Ariel (1994) [41], forearc peridotite, backarc peridotite, and abyssal peridotite [19] are shown for comparison; (b)  $\text{Al}_2\text{O}_3$  versus  $\text{TiO}_2$  diagram after Kamenetsky et al. [42] for the studied chromites**

particularly Cs and Rb are similar to Mariana fore-arc and two Guatemala fore-arc serpentinites [45]. The REE patterns of studied peridotites have overall lower HREE abundances and display relatively flat REE to concave-up normalized chondrite-normalized REE patterns. These are similar to the serpentinites associated with Mid-ocean ridge and fore-arc, which have low REE concentrations and display concave-up pattern [45].

The analyzed serpentine minerals are mainly pseudomorphic serpentines with subordinate antigorite serpentines, which indicate that the parent minerals were first retrogressed to form lizardite and chrysotile. Progressive metamorphism has recrystallized these minerals into antigorite.

The studied serpentinites have  $\text{Al}_2\text{O}_3$  concentrations (0.25–3.73 wt. %) are akin to oceanic and active margin peridotites and Pan-African serpentinites. The  $\text{Al}_2\text{O}_3$  and CaO depletion characterizes fore-arc peridotites

The chromites from study area have high Cr# (Cr# varies from 0.51 to 0.87) representing most probably the primary phase which is similar to chromian spinels in mantle-derived peridotites. The presence of podiform chromites in the studied serpentinites is considered to be typical of supra-subduction ophiolites with Cr# similar to those of forearc ophiolites and boninite-derived chromites.

Qala en Nahal-Umm Saqata mantle peridotites formed in a forearc setting during the subduction initiation that developed as a result of southeastward dipping subduction zone and possibly represent ensimatic, thrust material after the collision of the Nubian-Arabian Shield with the older sialic continental Saharan Metacraton during the late Proterozoic, Pan-African tectono-thermal event.

#### Acknowledgement

These investigations were carried out supported by the Peoples' Friendship University of Russia (RUDN University), Moscow, Russia and the Faculty of Petroleum and Minerals, Al Neelain University, Sudan. The publication has been prepared with the support of the «RUDN University Program 5–100». To all we express our thanks and appreciations.

#### References

- Ghanem H., McAleer R. J., Jarrar G. H., Al Hseinat M., Whitehouse M.  $^{40}\text{Ar}/^{39}\text{Ar}$  and U-Pb SIMS zircon ages of Ediacaran dikes from the Arabian-Nubian Shield of south Jordan. *Precambrian Research*. 2020. Vol. 343. 105714.
- Kröner A. Ophiolites and the evolution of tectonic boundaries in the late Proterozoic Arabian–Nubian Shield of north-east Africa and Arabia. *Precambrian Research*. 1985. Vol. 27, No. 1–3. pp. 277–300.
- Stern R. J. Arc assembly and continental collision in the Neoproterozoic East African Orogen: Implications for the consolidation of Gondwanaland. *Annual Review of Earth and Planetary Sciences*. 1994. Vol. 22. pp. 319–351.
- Loizenbauer J., Wallbrecher E., Fritz H., Neumayer P., Khuddeir A. A. et al. Structural geology, single zircon ages and fluid inclusion studies of the Meatiq metamorphic core complex: implication for Neoproterozoic tectonics in the Eastern Desert of Egypt. *Precambrian Research*. 2001. Vol. 110, No. 1–4. pp. 357–383.
- Kusky T. M. Precambrian Ophiolites and Related Rocks: Introduction. *Developments in Precambrian Geology*. 2004. Vol. 13. pp. 1–35.
- Hassan M. A., Kotelnikov A. E., Abdullah E. A. Geochemistry and Geotectonic Setting of the Post-orogenic granites at Qala En Nahal-Um Saqata Area, Gedarif State, Sudan. *IOP Conference Series: Earth and Environmental Science*. 2020. Vol. 459, No. 3. 042032. DOI: 10.1088/1755-1315/459/4/042032
- Gansser A. The ophiolite mélangé, a world-wide problem on Tethyan examples. *Eclogae Geologicae Helveticae*. 1974. Vol. 67. p. 479–507.
- Azer M. K., Khalil A. E. S. Petrological and mineralogical studies of Pan-African serpentinites at Bir Al-Edeid area, central Eastern Desert, Egypt. *Journal of African Earth Sciences*. 2005. Vol. 43, No. 5. pp. 525–536.
- Wicks F. J., Whittaker E. J. W. Serpentine textures and serpentinization. *Canadian Mineralogist*. 1977. Vol. 15, No. 4. pp. 459–488.
- O'Hanley D. S. Serpentinities: Records of Tectonic and Petrological History. New York: Oxford University Press, 1996. 277 p.
- Coleman R. G. Ophiolites. Berlin: Springer-Verlag, 1977. 229 p.
- Li X.-P., Rahn M., Buche K. Serpentinities of the Zermatt-Saas ophiolite complex and their texture evolution. *Journal of metamorphic Geology*. 2004. Vol. 22, No. 3. pp. 159–177.
- McDonough W. F., Sun S. S. Composition of the Earth. *Chemical Geology*. 1995. Vol. 120, No. 3–4. pp. 223–253.
- Boynton W. V. Cosmochemistry of the Rare Earth Elements: Meteorite Studies. *Rare Earth Element Geochemistry*. P. Henderson (Ed.). Amsterdam: Elsevier, 1984. Vol. 2. pp. 63–114.



15. Proenza J. A., Ortega-Gutierrez F., Camprubi A., Tritlla J., Elias-Herrera M., Reyes-Salas M. Paleozoic serpentinites enclosed chromitites from Tehuizingo (Acatlán Complex, southern Mexico): a petrological and mineralogical study. *Journal of South American Earth Sciences*. 2004. Vol. 16, No. 8. pp. 649–666.
16. Coleman R. G. Plate tectonic emplacement of upper mantle-peridotite along continental edges. *Journal of Geological Research*. 1971. Vol. 76, No. 5. pp. 1212–1222.
17. Dungan M. A. A microprobe study of antigorite and some serpentine pseudomorphs. *Canadian Mineralogist*. 1979. Vol. 17, No. 4. pp. 711–784.
18. Wicks F. J., Plant A. G. Electron microprobe and X-ray microbeam studies of serpentine textures. *Canadian Mineralogist*. 1979. Vol. 17, No. 4. pp. 785–830.
19. Dick H. J. B., Bullen T. Chromian spinel as a petrogenetic indicator in abyssal and alpine-type peridotites and spatially related lavas. *Contributions to Mineralogy and Petrology*. 1984. Vol. 86. pp. 54–76.
20. Barnes S. J. Chromite in Komatiites, II. Modification during Greenschist to Mid-Amphibolite Facies Metamorphism. *Journal of Petrology*. 2000. Vol. 41, No. 3. pp. 387–409.
21. Leblanc M., Dupuy C., Cassard D., Noutte J., Nicolas A. Essai sur la genèse des corps podiformes de chromite dans les peridotites ophiolitiques: étude des chromites de Nouvelle. *Ophiolites Proceedings International Symposium Cyprus. Geological Survey Department, Cyprus Publication*. 1980. pp. 691–701.
22. Roeder P. L. Chromite from the Fiery rain of Chondrules to the Kilauea iki lava lake. *Canadian Mineralogist*. 1994. Vol. 32, No. 4. pp. 729–746.
23. Bonavia F. F., Diella V., Ferrario A. Precambrian podiform chromitites from Kenticha Hill, southern Ethiopia. *Economic Geology*. 1993. Vol. 88, No. 1. pp. 198–202.
24. Arai S., Uesugi J., Ahmed A. H. Upper crustal podiform chromite from the northern Oman ophiolite as the stratigraphically shallowest chromite in ophiolite and its implication for Cr concentration. *Contributions to Mineralogy and Petrology*. 2004. Vol. 147, No. 2. pp. 145–154.
25. Ferrario A., Garuti G. Platinum-group minerals in chromite-rich horizons of the Niquelandia complex (central Goiás, Brazil). *Geo-Platinum*. 1987. Vol. 87. pp. 261–272.
26. Floyd P. A. Oceanic basalts. Blachie and Son Ltd., 1991. 455 p.
27. Bonatti E., Michael P. J. Mantle peridotites from continental rifts to oceanic basins to subduction zones. *Earth and Planetary Science Letters*. 1989. Vol. 91, No. 3–4. pp. 297–311.
28. El Bahariya G. A., Arai S. Petrology and origin of Pan-African serpentinites with particular reference to chromian spinel composition, Eastern Desert, Egypt: Implication for supra-subduction zone ophiolite. *3<sup>rd</sup> International Conference on the Geology of Africa*. Assiut University, Egypt. 2003. pp. 371–388.
29. Ishii T., Robinson P. T., Maekawa H., Fiske R. Petrological Studies of Peridotites from Diapiric Serpentine Seamounts in the Izu-Mariana Fore-arc, Leg 125. *Proceedings of the Ocean Drilling Program. Scientific Results*. 1992. Vol. 125. pp. 445–485.
30. Pearce J. A., Lippard S. J., Roberts S. Characteristics and tectonic significance of supra-subduction zone ophiolites. *Geological Society, Special Publication*. 1984. Vol. 16, pp. 77–94.
31. Arai S. Chemistry of chromian spinel in volcanic rocks as a potential guide to magma chemistry. *Mineralogical Magazine*. 1992. Vol. 56, No. 383. pp. 173–184.
32. Kahya A., Kuşçu M. Open System Condition Serpentinization of Host-rock Magnesite in Süleymaniye, Tutluca and Margi Region of Eskişehir, NW Turkey. *Universal Journal of Geoscience*. 2016. Vol. 4, No. 6. pp. 128–143.
33. Pober E., Faupl P. The chemistry of detrital chromite spinels and its implication for the geodynamic evolution of the eastern Alps. *33. Geologische Rundschau*. 1988. Vol. 77(3). pp. 641–670.
34. Abdel-Karim A. M., Ali S., Helmy H. M., El-Shafei S. A. A fore-arc setting of the Gerf ophiolite, Eastern Desert, Egypt: Evidence from mineral chemistry and geochemistry of ultramafites. *Lithos*. 2016. Vol. 263. pp. 52–65. DOI: 10.1016/j.lithos.2016.05.023
35. Dilek Y., Furnes H., Shallo M. Suprasubduction zone ophiolite formation along the periphery of Mesozoic Gondwana. *Gondwana Research*. 2007. Vol. 11, No. 4. pp. 453–475.
36. Farahat E. S. Neoproterozoic arc-back-arc system in the Central Eastern Desert of Egypt: Evidence from supra-subduction zone ophiolites. *Lithos*. 2010. Vol. 120, No. 3–4. pp. 293–308.
37. Pearce J. A. Supra-subduction zone ophiolites: The search for modern analogues. *Geological Society, Special Paper*. 2003. Vol. 373. pp. 269–294.
38. Zhou M. F., Robinson P. T. High-Cr and high-Al podiform chromitites, Western China: relationship to partial melting and melt/rock reaction in the upper mantle. *International Geology Reviews*. 1994. Vol. 36. pp. 678–686.
39. Proenza J., Gervilla F., Melgarejo J. C., Bodinier J.-L. Al- and Cr-rich chromitites from the Mayari-Baracoa Ophiolitic Belt (Eastern Cuba): consequence of interaction between volatile-rich melts and peridotites in suprasubduction mantle. *Economic Geology*. 1999. Vol. 94, No. 4. pp. 547–566.
40. Barnes S. J., Roeder P. L. The range of spinel compositions in terrestrial mafic and ultramafic rocks. *Journal of Petrology*. 2001. Vol. 42, No. 12. pp. 2279–2302.
41. Arai S. Characterization of spinel peridotites by olivine-spinel compositional relationships: review and interpretation. *Chemical Geology*. 1994. Vol. 113, No. 3–4. pp. 191–204.
42. Kamenetsky V. S., Crawford A. J., Meffre S. Factors controlling chemistry of magmatic spinel: an empirical study of associated olivine, Cr-spinel and melt inclusions from primitive rocks. *Journal of Petrology*. 2001. Vol. 42, No. 4. pp. 655–671.
43. Stolper E., Newman S. The role of water in the petrogenesis of Mariana trough magmas. *Earth and Planetary Science Letters*. 1994. Vol. 121, No. 3–4. pp. 293–325.
44. Keppler H. Constraints from partitioning experiments on the composition of subduction-zone fluids. *Nature*. 1996. Vol. 380. pp. 237–240.
45. Kodolányi J., Pettke T., Spandler C., Kamber B. S., Gmelin K. Geochemistry of Ocean Floor and Fore-arc Serpentinities: Constraints on the Ultramafic Input to Subduction Zones. *Journal of Petrology*. 2012. Vol. 53, No. 2. pp. 235–270. 